

Surface Modification of MWNTs with BA-MMA-GMA Terpolymer by Single-Step Grafting Technique

Ru Xia, Minghua Li, Yuchuan Zhang, Jiasheng Qian, Xiaoyou Yuan

The Key Laboratory of Environment-Friendly Polymer Materials of Anhui Province, School of Chemistry and Chemical Engineering, Anhui University, Hefei 230039, Anhui, People's Republic of China

Received 10 May 2009; accepted 29 March 2010

DOI 10.1002/app.32529

Published online 21 July 2010 in Wiley Online Library (wileyonlinelibrary.com).

ABSTRACT: In this article, a facile strategy was developed to prepare BA-MMA-GMA/MWNTs (multiwalled carbon nanotubes) hybrid nanoparticles as nanofillers in rubber by single-step grafting technique. First, a new macromolecular surface modifier butyl acrylate (BA)- α -methyl methacrylate(MMA)-glycidyl methacrylate (GMA) terpolymer was synthesized via radical copolymerization. Afterward, this terpolymer modifier was covalently grafted onto the surface of crude MWNTs by single-step grafting technique. The structure, surface properties, and thermal stability of modified MWNTs were systematically investi-

gated by FTIR, TGA, and TEM. FTIR results showed that BA-MMA-GMA terpolymer was successfully grafted onto the surface of MWNTs. TGA indicated that the optimum mass fraction of macromolecular modifier coated on the surface of MWNTs was 9 wt %. TEM images revealed that an organic coating layer was formed and the modified MWNTs showed good dispersibility in acetone. © 2010 Wiley Periodicals, Inc. *J Appl Polym Sci* 119: 282–289, 2011

Key words: BA-MMA-GMA terpolymer; macromolecular modifier; MWNTs; surface modification

INTRODUCTION

Since their discovery in 1991, carbon nanotubes (CNTs) have been a hot research topic because of their unique architecture, good mechanical properties, and broad-based potential applications.^{1,2} The mechanical properties and high aspect ratios of CNTs suggest that they can be used as reinforcing fillers in nanocomposites for which stiffness, strength, and weight are the important considerations.^{3–6} When CNTs are applied in preparing polymer nanocomposites,^{7–15} they must be available in large volumes at low cost and dispersible in the bulk material matrix, also the strong interactions between CNTs and the surrounding matrix should be formed. However, a number of challenges have to be met before nanotubes can be exploited for most of these notional applications that include expanding synthetic approaches to large-scale production and developing chemical techniques for manipulating CNTs.¹⁶ Commonly, single-walled carbon nanotubes (SWNTs) exhibit simpler structures and are more easily controllable compared with mul-

tiwalled carbon nanotubes (MWNTs). Therefore, most of the previous academic studies on CNTs including functional chemistry focused on SWNTs. The high price of SWNTs severely restricts its commercial applications. Fortunately, MWNTs have been realized in industrial production in recent years.^{17,18}

More recently, the “grafting from” approach has been developed to functionalize MWNTs and SWNTs,^{19–23} by which polymer chains can be *in situ* grafted more densely onto the convex walls of CNTs. Initially, by *in situ* radical polymerization, polystyrene was grafted onto the MWNTs by Shaffer.²⁴ The “grafting from” approach relies on the immobilization of initiators at the surface of CNTs, followed by *in situ* surface-initiated polymerization to generate polymer chains. Initiators for the controlled free radical polymerization of butyl methacrylate, methyl methacrylate, *N*-isopropylacrylamide, and styrene by atom transfer radical polymerization (ATRP) and reversible addition-fragmentation chain transfer (RAFT) have also been covalently attached to the CNTs' surface.^{21,25–32} The “grafting to” technique involves the bonding of preformed end functionalized polymer chains to the surface of CNTs.^{33–36} Whereas, the forementioned designs for the functionalization of CNTs usually consist of multistep syntheses. Sometimes, the preparation ways are rigorous and time-consuming, such as *in situ* radical polymerization,^{31,35,37,38} polycondensation,³⁹ living anionic polymerization.²¹ The most obvious drawback is that the prepared carbon nanotube composites are only on a milligram scale. This precludes their widespread applications, such as blending with conventional

Correspondence to: Y. Zhang (yuchuanzhang1946@126.com).

Contract grant sponsor: Chinese National Key Technology R&D Program; contract grant number: 2007BAE22B02.

Contract grant sponsor: Scientific Research Foundation for Ph.D. of Anhui University.

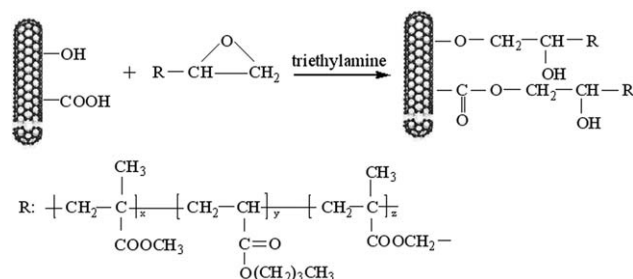


Figure 2 The single-step grafting route of BA-MMA-GMA / MWNTs Hybrid Nanoparticles.

deionized water to remove the solvent and the excess acid from this solution. The resulting materials were dried overnight at 100°C in a thermostat oven.

Titration

The titration procedure is exemplified below for the sodium bicarbonate analysis of carboxylic groups of MWNTs (MWNTs-COOH). A back titration was used to ensure the reliability of the results.

Forward titration

MWNTs-COOH + NaHCO₃ (excess) → MWNTs-COO⁻Na⁺ + NaHCO₃ (determined by titration)

Backward titration

MWNTs-COO⁻Na⁺ + HCl (excess) → MWNTs-COOH + HCl (determined by titration)

The calculating formula of carboxylic groups' content is shown below.

$$C = (N_{-\text{COOH}}/N_C) * 100\%$$

(C: The content of -COOH, %; N_{-COOH}: The content of -COOH on the surface of MWNTs, mol; N_C = M_C/12, The number of moles of carbons in the MWNTs, mol)

Preparation of BA-MMA-GMA / MWNTs hybrid nanoparticles

Optimum crude MWNTs nanopowders were dispersed in acetone, and a certain amount of (3–15% of total mass) macromolecular modifier (BA-MMA-GMA terpolymer) and triethylamine as catalyst were added into the flask, mixing round with high speed at 70°C for 2.5 h. Then the above reactants were titrated with HCl. The products were dried overnight at 50°C in vacuum and finally were crushed into powder. Figure 2 presents the single-step grafting route.

Characterization of MWNTs

Crude MWNTs and modified MWNTs were investigated by FT-IR (Neuxs-830, Nicolet, USA), TEM (JEM-100SX, TEOL, Japan) and TGA (Pyris-1, PE).

RESULTS AND DISCUSSION

Characterization of BA-MMA-GMA terpolymer by FTIR

FTIR testing was performed using Neuxs-830 to identify and characterize the structure of the terpolymer BA-MMA-GMA. It can be seen from Figure 6(c) that the peak 1732 cm⁻¹ is related to C=O stretching vibration mode, and the peaks at 2955 cm⁻¹ are related to -CH₂, -CH₃ asymmetric stretching mode. The peaks at 1462 cm⁻¹ and 1377 cm⁻¹ are, respectively, related to -CH₂- symmetric and asymmetric bending vibration. The band appears at 2880 cm⁻¹ corresponds to the stretching mode of -CH- in the epoxy group. We observed a broad peak centered 3500 cm⁻¹ corresponding to O-H stretching. The skeleton vibration absorption of epoxy group is at 1250 cm⁻¹ and the asymmetric stretching absorption of epoxy ring is at 957 cm⁻¹. These peaks are the characteristic peaks of terpolymer BA-MMA-GMA synthesized.

¹H-NMR and ¹³C-NMR analysis

¹H-NMR spectra of the terpolymer BA-MMA-GMA (as shown in Fig. 3) was obtained on an AVANCE 400 nuclear magnetic resonance spectrometer, using TMS as internal reference and deuterated acetone (CD₃COCD₃) as solvent. ¹H band for -CH₂- in the epoxy group -CH(O)CH₂ is 4.02 ppm and -COOCH₂- in GMA structural unit is 3.70 ppm. The peak assigned to -CH- in the epoxy group -CH(O)CH₂ is observed at 2.95 ppm. This indicates the existence of GMA structural unit in the

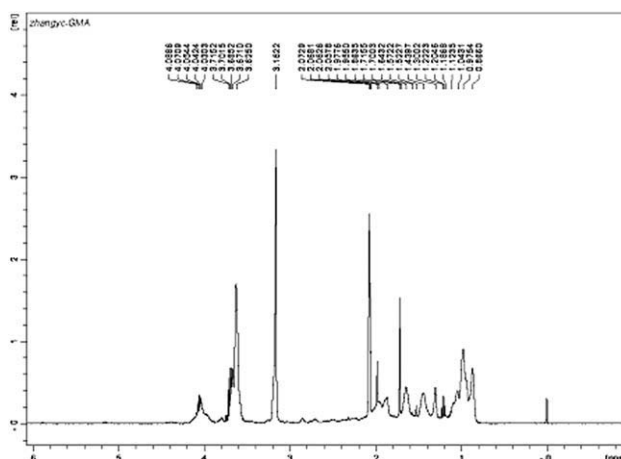


Figure 3 ¹H-NMR spectrum of BA-MMA-GMA.

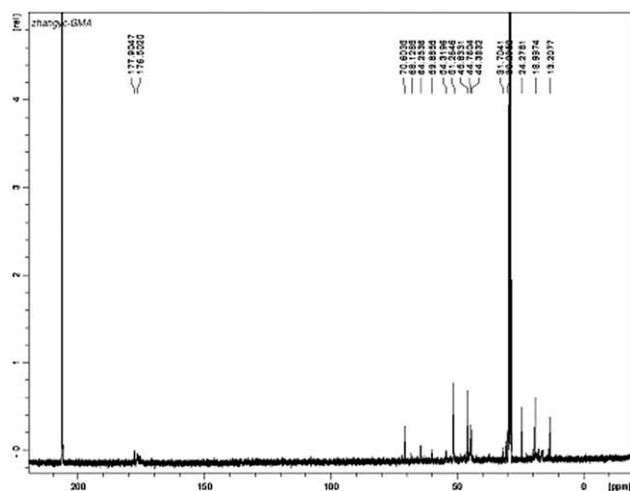


Figure 4 ^{13}C -NMR spectrum of BA-MMA-GMA.

terpolymer product. The methylene protons which are in the main chain resonate at 1.62 ppm and $-\text{CH}_3$ side group $-\text{COOCH}_2\text{CH}_2\text{CH}_2\text{CH}_3$ resonate at 1.42 ppm and $-\text{CH}_3$ side group which is in MMA structural unit absorb in the chemical shift range from 0.85 to 0.96. $\delta = 2.04$ is assigned to $>\text{CH}(\text{C}=\text{O})-$ in the BA unit.

The terpolymer structure is also confirmed by ^{13}C -NMR spectroscopy (as shown in Figure 4). All peaks in the spectrum clearly corresponded to proposed structure. The peak assigned to the $-\text{COO}-$ is observed at 175–177 ppm, and the $-\text{OCH}_2$ is observed at 64 ppm and $-\text{CH}_3$, $-\text{CH}_2-$, $-\text{CH}<$ are observed at 0–60 ppm.

The ^1H -NMR and ^{13}C -NMR results further demonstrate that the synthesized product is terpolymer BA-MMA-GMA, which is consistent with the FTIR results.

Titration results of different oxidation time

According to the references, the surface of MWNTs can be easily oxidized with the mixed concentrated nitric acid and sulfuric acid to form carboxyl groups. So we compared the carboxyl group content of crude MWNTs with that of MWNTs samples being oxidized for different time. The mole percentages of the MWNTs-COOH (MPM) groups are calculated by the formula in Titration section. Figure 5 shows the titration results of different oxidation time. The mole percentage of the MWNTs-COOH groups decreased after 16 h of oxidation. This is because the esterification reaction of carboxylic acid groups with the hydroxyl groups on the surface of the MWNTs in the presence of strong acid. The mole percentage of the MWNTs-COOH groups of the oxidized MWNTs for 16 h is the highest value (4.13%) among all the oxidated MWNTs samples by acid-base titration, only 0.63% higher than that of crude MWNTs

(3.50%). So, in this article, we skip the MWNTs oxidation process and use the crude MWNTs directly to carry out the surface modification.

FTIR characterization of functionalized MWNTs

Fourier transform infrared spectroscopy (FTIR) was utilized to characterize the changes of MWNTs after being modified with BA-MMA-GMA terpolymer, as shown in Figure 6. A broad peak at 1096 cm^{-1} in Figure 6(a) is identified as the C–O stretching mode, indicating the presence of carboxyl groups in the crude MWNTs. The peak at 1721 cm^{-1} in Figure 6(b) can be assigned to the stretching mode of carbonyl groups, indicating the presence of BA-MMA-GMA terpolymer chains in MWNTs. Figure 6(a) show minimal C=O stretch as we used the much larger diameter multiwalled CNTs (MWNTs).⁴⁷ In addition, a broad shoulder band in the $3350\text{--}3600\text{ cm}^{-1}$ region is attributed not only to the presence of hydroxyethyl groups in the crude MWNTs and modified MWNTs containing $-\text{OH}$ moieties but also to traces of water in the KBr pellet used for the analysis, which is inaccessible to be fully removed.⁴⁸ Meanwhile, the amount of hydroxyethyl groups in modified MWNTs has reduced owing to reaction of many hydroxyethyl groups with BA-MMA-GMA terpolymer. Carbonyl peaks have also been observed near 1630 cm^{-1} in modified MWNTs as shown in Figure 6(b). The peaks at 2930 cm^{-1} and 2852 cm^{-1} in Figure 6(b) correspond to the methylene and methenyl groups. These peaks are the characteristic peaks of BA-MMA-GMA terpolymer as shown in Figure 6(c).

These proved that the macromolecular modifier tightly absorbed at the surface of MWNTs by chemisorption and it is still exist in the modified powders even after being extracted by Soxhlet extractor among acetone.

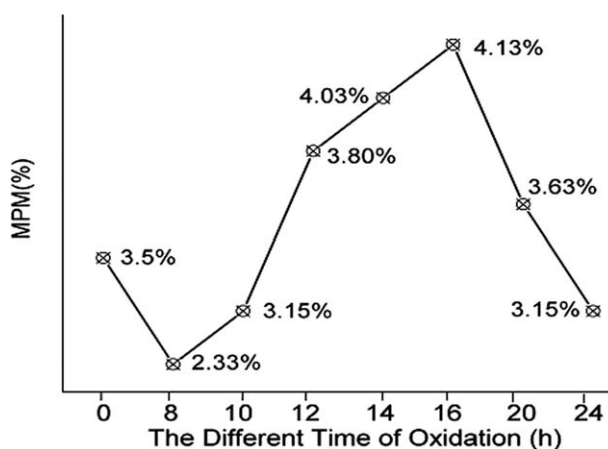


Figure 5 Titration results of different oxidation time.

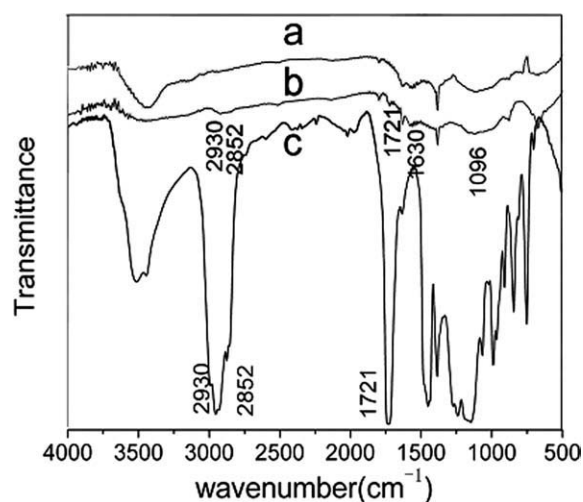


Figure 6 FTIR spectra of (a) the crude MWNTs, (b) modified MWNTs by Soxhlet extraction, (c) BA-MMA-GMA terpolymer.

TGA measurements

It is known that the defunctionalization of MWNTs can be realized by thermal decomposition, thermal gravity analysis (TGA) was used to determine the relative amount of grafted copolymer of MWNT-g-BA-MMA-GMA. Figure 7(a,b) show the TGA traces of crude MWNTs, BA-MMA-GMA terpolymer, and modified MWNTs with different mass ratio (wt%) of BA-MMA-GMA terpolymer and MWNTs under nitrogen. Figure 7(a) shows the weight loss corresponding to the crude MWNTs and BA-MMA-GMA terpolymer at 500°C under nitrogen is 2% and 99.88 wt %, respectively. The weight-loss region (100–250°C) in Figure 7(a) may be assigned to the decomposition of carboxyl and hydroxyl groups on the surface of MWNTs. From Table II we can conclude that the weight-loss region (250–500°C) in Figure 7(a) may be connected with the decomposition of the terpolymer backbone. Figure 7(b,c) display the weight loss of modified MWNTs with different wt % before and after Soxhlet extraction. The detailed datas of Figure 7(b,c) are exhibited in Table III.

Two weight-loss regions are also found for modified MWNTs sample. These shapes of TGA curve of modified MWNTs before and after Soxhlet extraction are similar with the decomposition of BA-MMA-GMA terpolymer. This suggests that the chains of terpolymer have linked by physical adsorption or chemical bonding to the surface of MWNTs.

According to the references,^{49–51} separation of the chemical bonding and physically adsorbed fractions is performed with the help of a Soxhlet extraction. So it is easy to differentiate between the chemical bonding and the unbound structures (physically adsorbed fraction) from Figure 7(b,c). The resulting fractions can be calculated with the following for-

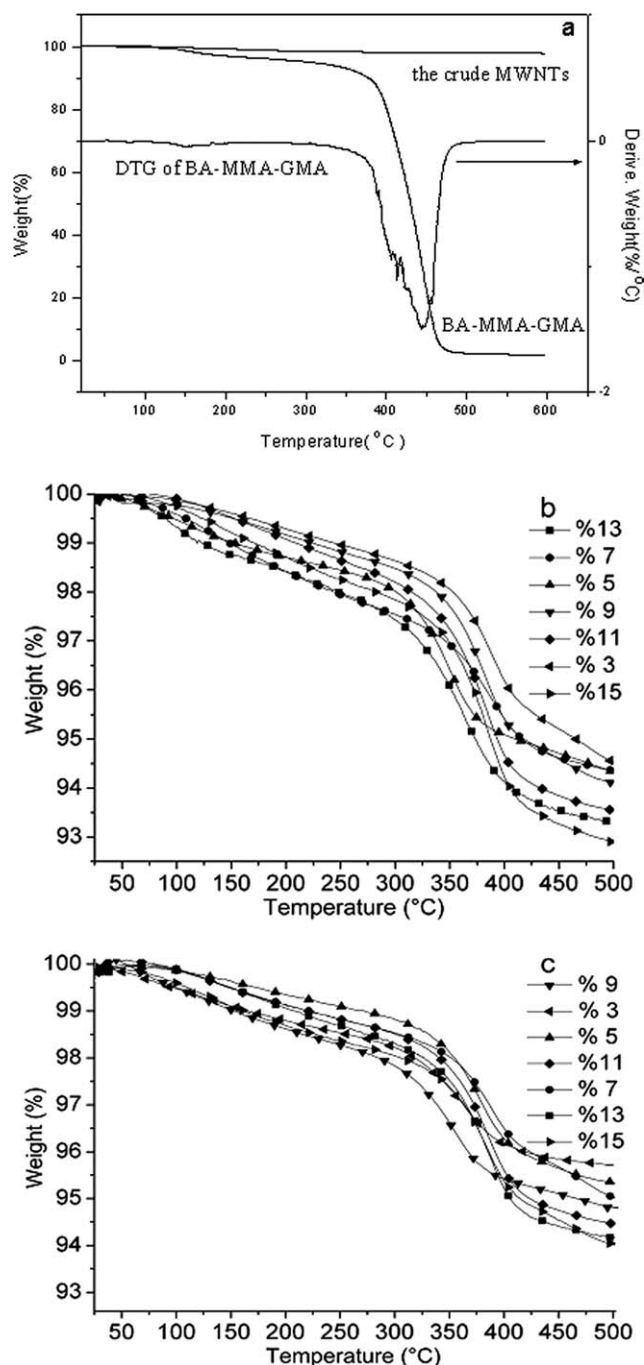


Figure 7 TGA curve of (a) crude MWNTs and BA-MMA-GMA terpolymer, (b) modified MWNTs, (c) modified MWNTs after Soxhlet extraction.

mula, which are listed in Table III. Figure 8 presents the relationship between chemical bonding fraction, CF, (PF) and terpolymer coated content.

TABLE II
TGA Data of BA-MMA-GMA and Crude MWNTs

Sample	T_i (°C)	T_{max} (°C)	T_t (°C)	Char yield (%)
BA-MMA-GMA	50	444	500	0.12 (500°C)
Crude MWNTs	100	135	250	98.0 (500°C)

TABLE III
TGA Data of Modified MWNTs

Sample (%)	Char yield (%) (500°C)		CF (%)	PF (%)
	A (Before Soxhlet extraction)	B (After Soxhlet extraction)		
3	95.01	95.90	70.23	29.77
5	94.68	95.50	75.30	24.70
7	94.33	95.20	76.30	23.70
9	94.00	94.45	88.75	11.25
11	93.55	94.50	78.65	21.35
13	93.09	94.46	72.09	27.91
15	92.89	94.35	71.43	28.57

$$CF = (M-B)/(M-A)$$

$$PF = 1 - CF$$

CF: Fraction of chemical bonding

PF: Fraction of physical adsorption.

M: Char yield (%) of native nanoparticles at X°C

A: Char yield (%) of modified nanoparticles before Soxhlet extraction at X°C

B: Char yield (%) of modified nanoparticles after Soxhlet extraction at X°C

As can be seen in Figure 8, with the increase of terpolymer coated content, the CF increases to reach its maximum and then declines. So, it can be conclude that the optimum mass fraction of macromolecular modifier coated on the surface of MWNTs is 9 wt %.

Dispersibility

Figure 9 shows the dispersibility of crude MWNTs and modified MWNTs in acetone. The dispersibility of the terpolymer modified MWNTs is much better than that of their totally physical mixture. The sample of physical mixture has obvious black sediment in acetone as shown in Figure 9. In contrast to crude MWNTs and MWNTs modified with different mass fraction of macromolecular modifier coated on the

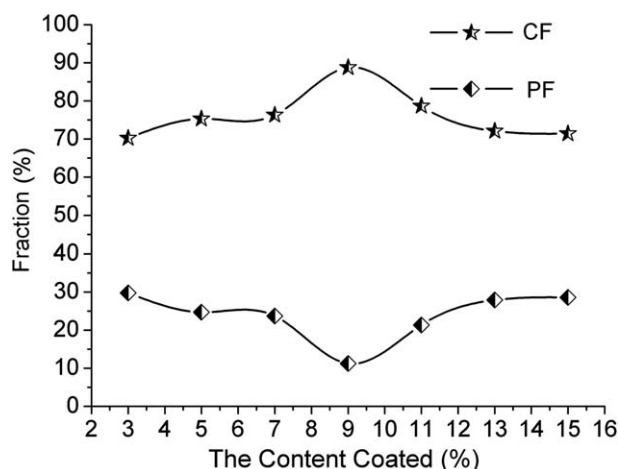


Figure 8 The curves of CF and PF.

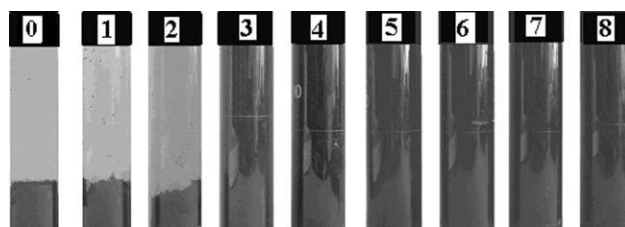


Figure 9 The solubility in acetone of crude MWNTs and modified MWNTs (0. physical mixture of MWNTs and terpolymer modifier; 1. crude MWNTs; 2. MWNTs modified with 3% terpolymer modifier; 3. 5% modifier; 4. 7% modifier; 5. 9% modifier; 6. 11% modifier; 7. 13% modifier; 8. 15% modifier).

surface of MWNTs, the crude MWNTs is insoluble, while 5–15 wt % modified MWNTs can be easily dispersed in acetone, and no sedimentation is observed more than 3 months. This suggests that functionalized MWNTs have excellent solubility in acetone. The reason that 3 wt % functionalized MWNTs prepared has black sediment may be the content of macromolecular modifier is too little to bring mutual exclusion and steric hindrance effect.

TEM

Figure 10 displays the TEM photographs of crude MWNTs and modified MWNTs suspensions in acetone which were prepared with ultrasonic vibrating method. To represent detailed morphological information of the specimens, different magnifications were utilized for samples. The obvious agglomeration can be seen in the photograph of crude MWNTs in Figure 10(a) and the homogeneous dispersion can be seen in the photograph of modified MWNTs in Figure 10(b). In the TEM photographs of Figure 10(b2), the terpolymer layers are clearly shown as the gray area, which are coated on the surface of MWNTs and reduce the agglomerations. This suggests that physical bonding or chemical bonding have been modified successfully by BA-MMA-GMA terpolymer. The molecular chains of macromolecular modifier which connected with the surface of crude MWNTs brought mutual exclusion and steric hindrance effect, thus the surface free energy reduced correspondingly and the agglomeration was controlled effectively.

CONCLUSIONS

A novel macromolecular modifier BA-MMA-GMA terpolymer was synthesized and it can be used to modify the MWNTs to prepare BA-MMA-GMA/MWNTs hybrid nanoparticles by single-step grafting technique. The results show that the optimum mass fraction of macromolecular modifier coated on the surface of MWNTs is 9 wt %. Some organic coating

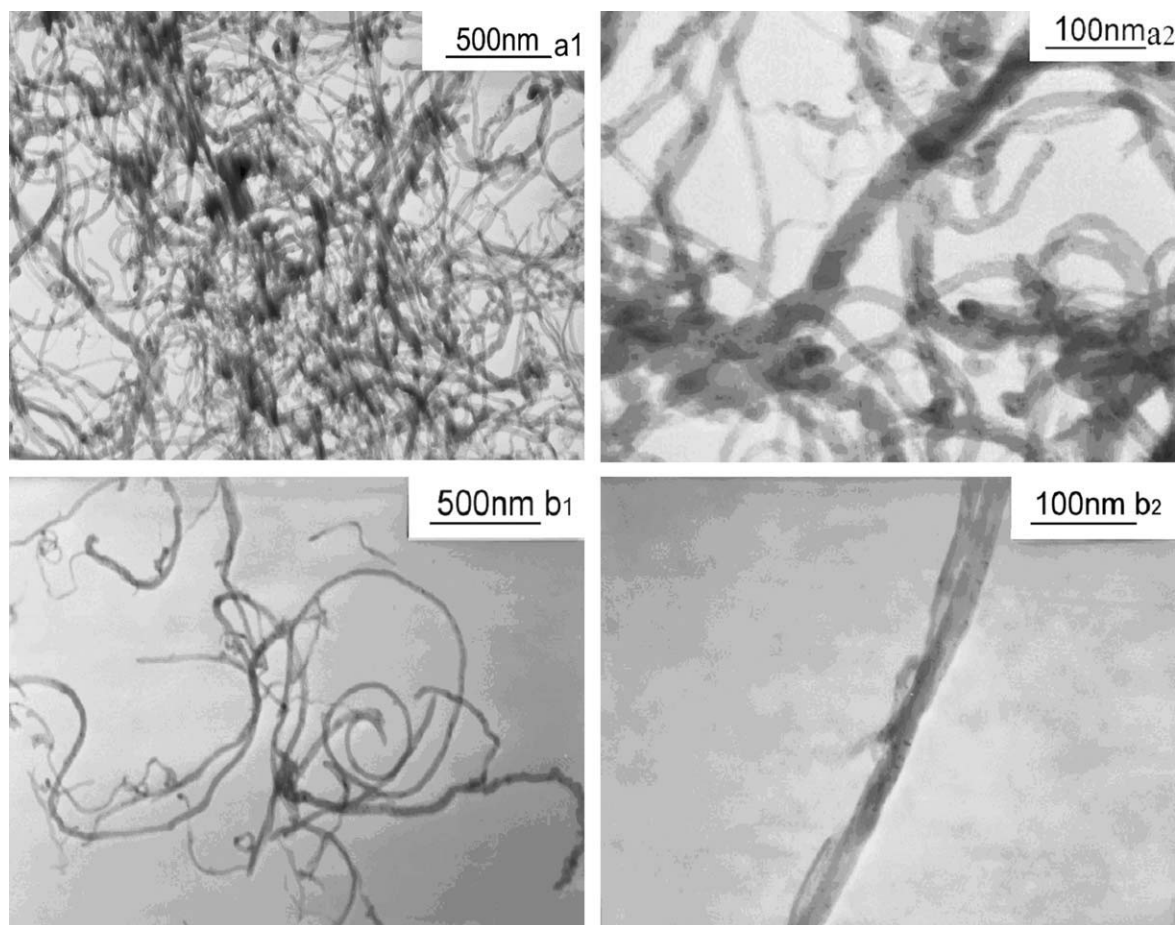


Figure 10 TEM micrographs of (a) crude MWNTs (b) modified MWNTs, showing different morphologies.

layer formed on the surface of MWTNs, and chemical bond combination happens between BA-MMA-GMA terpolymer and MWNTs surface. Modified MWNTs possesses good dispersibility in some organic solvents such as acetone, alcohol, toluene, THF, etc.

References

- Baughman, R. H.; Zakhidov, A. A.; De Heer, W. A. *Science* 2002, 297, 787.
- Tasis, D.; Tagmatarchis, N.; Bianco, A.; Prato, M. *Chem Rev* 2006, 106, 1105.
- Vaia, R. A.; Wagner, H. D. *Mater Today* 2004, 7, 32.
- Breuer, O.; Sunderaraj, U. *Polym Compos* 2004, 25, 630.
- Dyke, C. A.; Tour, J. M. *J Phys Chem A* 2004, 51, 11151.
- Tasis, D.; Tagmatarchis, N.; Georgakilas, V.; Prato, M. *Chem Eur J* 2003, 9, 4000.
- Geng, H. Z.; Rosen, R.; Zheng, B.; Shimoda, H.; Fleming, L.; Liu, J. Z. *Adv Mater* 2002, 14, 1387.
- Qian, D.; Dickey, E. C.; Andrews, R.; Rantell T. *Appl Phys Lett* 2000, 76, 2868.
- Cadek, M.; Coleman, J. N.; Barron, V. Hedicke, K.; Blau, W. J. *Appl Phys Lett* 2002, 81, 5123.
- Zhang, W. D.; Shen, L.; Phang, I. Y.; Liu, T. *Macromolecules* 2004, 37, 256.
- Zhang, X. F.; Liu, T.; Sreekumar, T. V.; Kumar, S.; Moore, V. C.; Hauge, R. H.; Smalley, R. E. *Nano Lett* 2003, 3, 1285.
- Frogley, M. D.; Ravich, D.; Wagner, H. D. *Compos Sci Technol* 2003, 63, 1647.
- Lau, K. T.; Hui, D. *Carbon* 2002, 40, 1605.
- Penumadu, D.; Dutta, A.; Pharr, G.; Files, B. *J Mater Res* 2003, 18, 1849.
- Gojny, F.; Wichmann, M.; Kopke, U.; Fiedler, B.; Schulte, K. *Compos Sci Technol* 2004, 64, 2363.
- Hirsch, A. *Angew Chem Int Ed* 2002, 41, 1853.
- Dalton, A. B.; Collins, S.; Razal, J.; Munoz, E.; Ebron, V. H.; Kim, B. G.; Coleman, J. N.; Ferraris, J. P.; Baughm, R. H. *Mater Chem* 2004, 14, 1.
- Kong, H.; Gao, C.; Yan, D. *Macromolecules* 2004, 37, 4022.
- Coleman, K. S.; Baily, S. R.; Fogden, S.; Green, M. L. H. *J Am Chem Soc* 2003, 125, 8722.
- Wu, W.; Zhang, S.; Li, Y.; Li, J.; Liu, L.; Qin, Y.; Guo, Z. X.; Dai, L.; Ye, C.; Zhu, D. *Macromolecules* 2003, 36, 6286.
- Viswanathan, G.; Chakrapani, N.; Yang, H.; Wei, B.; Chung, H.; Cho, K.; Ryu, C. Y.; Ajayan, P. M. *J Am Chem Soc* 2003, 125, 9258.
- Chen, S.; Wu, G.; Liu, Y.; Long, D. W. *Macromolecules* 2006, 39, 330.
- Stephenson, J. J.; Sadana, A. K.; Higginbotham, A. L.; Tour, J. M. *Chem Mater* 2006, 18, 4658.
- Shaffer, M. S. P.; Koziol, K. *Chem Commun* 2002, 18, 2074.
- Qin, S. H.; Qin, D. H.; Ford, W. T.; Resasco, D. E.; Herrera, J. *J Am Chem Soc* 2004, 126, 170.
- Xu, Y.; Gao, C.; Kong, H.; Yan D.; Jin, Y. Z.; Watts, P. C. P. *Macromolecules* 2004, 37, 8846.
- Gao, C.; Muthukrishnan, S.; Li, W. W.; Yuan, J. Y.; Xu, Y. Y.; Muler, A. H. E. *Macromolecules* 2007, 40, 1803.

28. Chen, S. M.; Shen, W. M.; Wu, G. Z.; Chen, D. Y.; Jiang, M. *Chem Phys Lett* 2005, 402, 312.
29. Baskaran, D.; Mays, J. W.; Bratcher, M. S. *Angew Chem Int Ed* 2004, 43, 2138.
30. Kong, H.; Gao, C.; Yan, D. Y. *J Am Chem Soc* 2004, 126, 412.
31. Pei, X.; Hao, J.; Liu, W. *Phys Chem C* 2007, 111, 2947.
32. Park, S. J.; Cho, M. S.; Lim, S. T.; Choi, H. J.; Jhon, M. S. *Macromol Rapid Commun* 2003, 24, 1070.
33. Hong, C. Y.; You, Y. Z.; Pan, C. Y. *Chem Mater* 2005, 17, 2247.
34. Qin, S. H.; Qin, D. H.; Ford, W. T.; Resasco, D. E.; Herrera, J. E. *Macromolecules* 2004, 37, 752.
35. Lou, X. D.; Detrembleur, C.; Pagnouille, C.; Jerome, R.; Bocharova, V.; Kiriya, A.; Stamm, M. *Adv Mater* 2004, 16, 2123.
36. Liu, Y. Q.; Yao, Z.; Adronov, A. *Macromolecules* 2005, 38, 1172.
37. Shaffer, M. S. P.; Koziol, K. *Chem Commun* 2002, 2074.
38. Hong, C. Y.; You, Y. Z.; Wu, D. C.; Liu, Y.; Pan, C. Y. *Macromolecules* 2005, 38, 2606.
39. Gao, C.; Jin, Y. Z.; Kong, H.; Witby, R. L. D.; Acquah, S. F. A.; Chen, G. Y.; Qian, H.; Hartschuh, A.; Silva, S. R. P.; Henley, S.; Fearon, P.; Kroto, H. W.; Walton, D. R. M. *J Phys Chem B* 2005, 109, 11925.
40. Sano, M.; Kamino, A.; Okamura, J. *Langmuir* 2001, 17, 5125.
41. Zhao, B.; Hu, H.; Yu, A. P.; Perea, D.; Haddon, R. C. *J Am Chem Soc* 2005, 127, 8197.
42. Hu, H.; Ni, Y. C.; Mandal, S. K.; Zhao, B.; Haddon, R. C.; Pappas, V. *J Phys Chem B* 2005, 109, 4285.
43. Xia, R.; Zhang, Y. C.; Zhu, Q. R.; Qian, J. S.; Dong, Q. N.; Li, F. S. *J Appl Polym Sci* 2008, 107, 562.
44. Xia, R.; Li, M. H.; Zhang, Y. C.; Zhu, Q. R.; Qian, J. S. *J Appl Polym Sci* 2008, 107, 1100.
45. Zhang, S.; Qian, J. S.; Zhang, Y. C. *China Rubber Ind* 2008, 55, 734.
46. Chai, D. F.; Dong, Q. N.; Zhang, Y. C. *Chin J Syn Chem* 2008, 16, 318.
47. Majumder, M.; Chopra, N.; Hinds, B. J. *J Am Chem Soc* 2005, 127, 9062.
48. Yao, Z.; Braidy, N.; Botton, G. A.; Adronov, A. *J Am Chem Soc* 2003, 125, 16015.
49. Wibke, D.; Lars, N.; Gudrun, S. N. *Macromol Symp* 2007, 259, 421.
50. Sabzi, M.; Mirabedini, S. M.; Zohuriaan-Mehr, J.; Atai, M. *Prog Org Coatgs* 2009, 65, 222.
51. Tang, E. J.; Cheng, G. X.; Ma, X. L. *Appl Surf Sci* 2006, 252, 5227.